Physics Letters B 714 (2012) 246–250

Contents lists available at SciVerse ScienceDirect

Physics Letters B

www.elsevier.com/locate/physletb

Erosion of $N = 20$ shell in ^{33}Al investigated through the ground-state electric quadrupole moment

K. Shimada [a,1], H. Ueno [b,*], G. Neyens [c], K. Asahi [a], D.L. Balabanski [d], J.M. Daugas [e], M. Depuydt [c], M. De Rydt [c,2], L. Gaudefroy [e], S. Grévy [f,3], Y. Hasama [a], Y. Ichikawa [b], D. Kameda [b], P. Morel [e], T. Nagatomo [b,4], L. Perrot [g], Ch. Stodel [f], J.-C. Thomas [f], Y. Utsuno [h], W. Vanderheijden [c], N. Vermeulen [c], P. Vingerhoets [c], E. Yagi [b], K. Yoshida [i], A. Yoshimi [b,5]

[a] Department of Physics, Tokyo Institute of Technology, 2-12-1 Oh-okayama, Meguro-ku, Tokyo 152-8551, Japan
[b] RIKEN Nishina Center, 2-1 Hirosawa, Wako, Saitama 351-0198, Japan
[c] Instituut voor Kern- en Stralingsfysica, KU Leuven, Celestijnenlaan 200D, B-3001 Leuven, Belgium
[d] Institute for Nuclear Research and Nuclear Energy, Bulgarian Academy of Sciences, BG-1784 Sofia, Bulgaria
[e] CEA, DAM, DIF, F-91297 Arpajon, France
[f] Grand Accélérateur National d'Ions Lourds, CEA/DSM-CNRS/IN2P3, BP 55027, F-14076 Caen Cedex 5, France
[g] Institut de Physique Nucléaire d'Orsay, 15 Rue G. Clemenceau, F-91406 Orsay, France
[h] Japan Atomic Energy Agency, Tokai-mura, Ibaraki 319-1195, Japan
[i] Department of Physics, Graduate School of Science and Technology, Niigata University, Niigata 950-2181, Japan

ARTICLE INFO

Article history:
Received 21 October 2011
Received in revised form 31 May 2012
Accepted 3 July 2012
Available online 17 July 2012
Editor: V. Metag

Keywords:
Electric quadrupole moment of ^{33}Al
β-NMR
Island of inversion
Shell model
Quasiparticle-vibration coupling model

ABSTRACT

Electric quadrupole moment Q of the ^{33}Al ground state has been measured by means of β-NMR spectroscopy using a spin-polarized ^{33}Al beam produced in a projectile fragmentation reaction. The obtained Q moment, $|Q_{\mathrm{exp}}(^{33}\mathrm{Al})| = 132(16)$ *emb*, shows a significant excess from the prediction of shell model calculations within the *sd* shell. The result indicates sizable admixing of *pf* intruder configurations in the ground state, demonstrating that the $N = 20$ shell closure certainly erodes in ^{33}Al, a nucleus located on the border of the *island of inversion*. Comparison was made with predictions of the Monte Carlo shell model, and also a particle-vibration coupling model treating the neutron pairing correlations in the ground state of ^{33}Al. Again, a significant admixture of *pf* intruder configurations to the ^{33}Al ground state was needed in both theoretical approaches to explain the observed large Q.

The region of the nuclear chart consisting of neutron-rich Ne, Na, and Mg isotopes around the neutron number $N = 20$ is known as the *island of inversion*, where the nuclear ground states are dominated by intruder configurations from the upper *pf* orbits and are considerably deformed [1]. Among the $N = 20$ isotones, numerous studies have been conducted for nuclei inside the *island of inversion* [2–6], but not much effort has been devoted to their neighbors, such as ^{33}Al. In the systematic mass measurements around $A \simeq 32$ [7], from which the anomalously tight binding of nuclei in this region was recognized, no remarkable feature was found for ^{33}Al [8].

Nuclear magnetic dipole (μ) and electric quadrupole (Q) moments are sensitive respectively to the nucleon configuration and to the E2 collectivity. Recently, the μ-moment measurement of the ^{33}Al ground state has been reported [9], where it is suggested that the mixture of *pf* intruder configurations could explain an observed difference, $\Delta\mu(^{33}\mathrm{Al}) = 3.9\%$, between the experimental $\mu(^{33}\mathrm{Al})$ moment and a shell-model calculation within the *sd* model space. This observation contradicts a β–γ spectroscopic work carried out on ^{33}Al [10], which reports that the observed β-decay properties of ^{33}Al are well described by the *sd* shell model

* Corresponding author.
E-mail address: ueno@riken.jp (H. Ueno).

[1] Present address: Cyclotron and Radioisotope Center, Tohoku University, 6-3 Aoba, Aramaki, Aoba-ku, Sendai, Miyagi 980-8578, Japan.
[2] Present address: Institut de Physique Nucléaire, CNRS/IN2P3, Université Claude Bernard Lyon 1, F-69622 Villeurbanne Cedex, France.
[3] Present address: Centre d'Etudes Nucléaires de Bordeaux-Gradignan, Université de Bordeaux 1 – UMR 5797 CNRS/IN2P3, Chemin du Solarium, BP 120, 33175 Gradignan Cedex, France.
[4] Present address: Institute of Materials Structure Science, High Energy Accelerator Research Organization, Ibaraki 319-1106, Japan.
[5] Present address: Research Core for Extreme Quantum World, Okayama University, Okayama 700-8530, Japan.

0370-2693
http://dx.doi.org/10.1016/j.physletb.2012.07.030

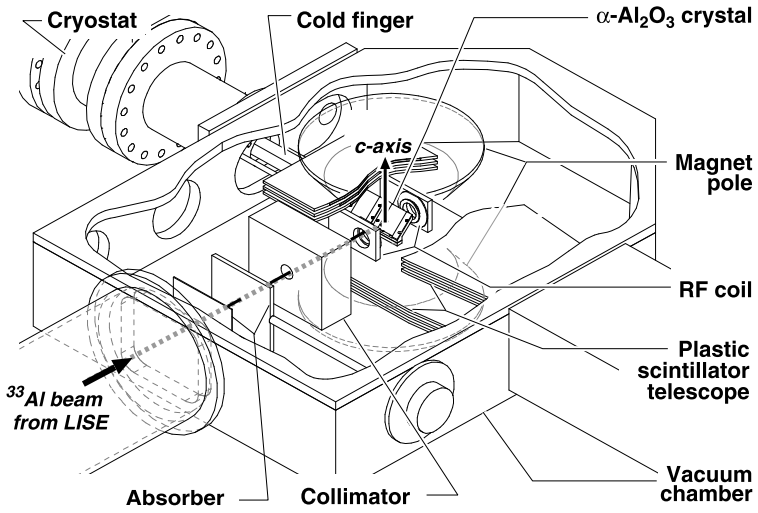

Fig. 1. Schematic layout of the β-NMR apparatus. Details are given in Ref. [23].

calculations, suggesting that the ground state of this nucleus lies primarily outside of the *island of inversion*. Contrary to this, a β-decay study [11] indicates a sizable admixture of intruder configurations in the ^{33}Al ground state.

It would be worth noting here that, although most of theoretical analyses of the nuclear structures arising in the *island of inversion* are based on the consideration of strong nuclear deformations [7], the possibility of other mechanisms may also be important. For instance, the importance of the neutron pairing correlation instead of nuclear deformation [12] and a picture of quadrupole-shape fluctuations which dominate both the ground and the excited $I^\pi = 0^+$ states [13] were proposed to describe the ^{32}Mg nucleus.

In the present work, the ground-state Q moment of ^{33}Al ($I^\pi = 5/2^+$, $T_{1/2} = 41.7(2)$ ms) has been measured by means of β ray-detected nuclear magnetic resonance (β-NMR) [14] with incorporation of the technique of fragmentation-induced spin-polarized radioactive isotope beams [15,16]. Comparing the obtained $Q(^{33}\mathrm{Al})$ with those reported for other neutron-rich aluminum isotopes, possible evolution of nuclear structure around ^{33}Al will be signified due to its high sensitivity to the collectivity such as deformation and paring correlation. So far, the μ moments of $^{30-34}$Al [9,17–19] and the Q moments of ^{31,32}Al [20–22] have been measured.

The experiment was carried out at the Grand Accélérateur National d'Ions Lourds (GANIL). A beam of ^{33}Al was obtained from the fragmentation of ^{36}S projectiles at $E = 77.5A$ MeV on a 0.22 g/cm^2 thick ^{9}Be target. In order to produce spin-polarized ^{33}Al, fragments emitted at finite angles, $\theta_{\mathrm{Lab}} = 1$–$3^\circ$, from the primary beam direction were introduced to the fragment separator LISE. The primary beam was deflected by 2° with respect to the target located at the spectrometer entrance. A range of momenta $p/p_{\mathrm{b}} = 1.026$–1.041 was selected with slits placed at the momentum-dispersive intermediate focal plane. Here, $p_{\mathrm{b}} = 11.7$ GeV/c is the fragment momentum corresponding to the projectile velocity. With a 2 μA intensity of the primary $^{36}S^{16+}$ beam, LISE provided the beam of ^{33}Al with a purity of 75% and intensity of 1300 particles/s. The spin-polarized ^{33}Al fragments were transported to a β-NMR apparatus [23] located at the final focus of LISE, and were implanted in a stopper of hexagonal α-Al_2O_3 single crystal (corundum). A static magnetic field $B_0 = 497.62$ mT was applied to the stopper in order to preserve the ^{33}Al spin polarization. The layout of the β-NMR apparatus is shown in Fig. 1. The α-Al_2O_3 crystal was cut into a $25.5 \times 28 \times 1$ mm slab, and was mounted in a stopper chamber so that the c axis was oriented parallel to the B_0 field. The stopper was kept in vacuum and cooled to a temperature $T \simeq 80$ K to suppress the spin-lattice relaxation of ^{33}Al during the β-decay [20].

The Q moment interacts with an electric field gradient eq acting at the site of the implanted nucleus in a single crystal stopper. The eqQ interaction causes energy shifts in the individual Zeeman magnetic sublevels. Under the present situation of the experiment, where the angle between the c axis and the B_0 field was set at $\theta = 0^\circ$, the resonance frequency $\nu_{m,m+1}$ between magnetic sublevels m and $m+1$ ($m = -I, -I+1, \ldots, I-1$) of the nuclear spin $I = 5/2$ is given by

$$\begin{aligned}\nu_{m,m+1} &= \nu_{\mathrm{L}} - \nu_{\mathrm{Q}}\bigl(3\cos^2\theta - 1\bigr)\frac{3(2m+1)}{8I(2I-1)} \\ &= \nu_{\mathrm{L}} - \frac{3}{40}(2m+1)\nu_{\mathrm{Q}}, \end{aligned} \tag{1}$$

where ν_{L} denotes the Larmor frequency, $\nu_{\mathrm{Q}} = eqQ/h$ the quadrupole coupling constant, and eq the electric field gradient along the c axis. Q and h denote the Q moment and the Planck's constant, respectively. If the true value for ν_{Q} is inserted in Eq. (1), the application of an oscillating magnetic field B_1 whose frequency is swept across $\nu_{m,m+1}(\nu_{\mathrm{Q}})$ should lead to a reversal of the population between sublevels m and $m+1$ (the adiabatic fast passage technique (AFP) [24]). Application of a B_1 field having all these five ($= 2I$) different $\nu_{m,m+1}$ frequency components ensures that through scanning the single parameter ν_{Q}, the fulfillment of $\nu_{\mathrm{Q}} = eqQ(^{33}\mathrm{Al})/h$ could be detected through the simultaneous occurrence of all the $2I = 5$ resonances, which consequently leads to collective alteration of the spin polarization [20]. Note that the full reversal of spin requires a sequence of stepwise reversals between two contiguous sublevels. The B_1 field was applied in $I(2I+1) = 15$ steps in the same sequence as described in Ref. [25]. In each step the frequency ν was swept from $\nu_{m,m+1}(\nu_{\mathrm{Q}}{}^{\mathrm{lower}})$ to $\nu_{m,m+1}(\nu_{\mathrm{Q}}{}^{\mathrm{upper}})$ with $\nu_{\mathrm{Q}}{}^{\mathrm{lower}}$ and $\nu_{\mathrm{Q}}{}^{\mathrm{upper}}$ denoting the lower and upper bounds of the searched ν_{Q} region.

Thus, the ν_{Q} resonance was detected as a change in the β-ray asymmetry (we hereafter denote this technique of β-ray detected NMR spectroscopy in a non-cubic crystal by the β-NQR method). The β-rays emitted from the implanted ^{33}Al nuclei were detected with scintillator telescopes located above and below the stopper. They were housed inside the vacuum chamber, each consisting of three 1 mm-thick plastic scintillators. The up/down ratio R of the β-ray counts is written as

$$R = a\frac{1 + v/c \cdot A_\beta P}{1 - v/c \cdot A_\beta P} \simeq a(1 + 2A_\beta P), \tag{2}$$

where a is a constant factor representing asymmetries in the counter solid angles ($\Omega_\beta \approx 4\pi \times 0.22$ sr each) and efficiencies, v/c the velocity of the β particle, A_β the asymmetry parameter, and P the ^{33}Al nuclear spin polarization. The primary branch of the ^{33}Al β-decay is to the ground state of ^{33}Si with a branching ratio of ∼89% [10] and decay Q value $Q_\beta = 11.990$ MeV [26]. Since a β particle looses part of its energy in penetrating the materials around the stopper before entering the β-ray telescope, only those β particles with $E_\beta \gtrsim 1600$ keV [27] (or $v/c \gtrsim 0.97$) were counted. Thus, the ratio R in Eq. (2) is well approximated by the second expression setting $v/c \approx 1$. By taking a double ratio R/R_0, where R_0 is the value for R measured without the B_1 field, the change in the R/R_0 ratio of the β-ray yields upon the NQR is given as

$$\frac{R}{R_0} \simeq \frac{a(1 - 2A_\beta P)}{a(1 + 2A_\beta P)} \simeq 1 - 4A_\beta P, \tag{3}$$

if the fragment spin polarization is fully reversed from P to $-P$. Since the constant a is canceled out in Eq. (3), the alternation of the spin polarization can be detected as the deviation of R/R_0 from the unity. The resonance frequency is derived from the position of a peak or dip in the R/R_0 spectrum. The experiment was done with a pulsed beam with typical beam-on and beam-off periods of 20 and 109 ms, respectively. In the beam-off period, the sequence of the B_1-field for the nuclear magnetic resonance was applied in the first 9 ms duration, and then the β-rays were counted in the remaining 100 ms duration.

Fig. 2(a) shows a β-NMR spectrum obtained for ^{33}Al in a cubic Si crystal in runs prior to the NQR measurements, using the same apparatus and B_0 setting for the ν_L determination. The spectrum was analyzed based on a least-χ^2 fitting procedure with a Gaussian function

$$G_\sigma(\nu) = a\exp\left(-\frac{(\nu - \nu^{(0)})^2}{2\sigma^2}\right) + 1. \tag{4}$$

Here a and $\nu^{(0)}$ are the parameters that were varied during the fitting procedure, while σ was kept constant at values obtained from a numerical simulation, in which a time-dependent Schrödinger equation of the spin motion in the AFP spin reversal process was solved under the actual B_0 and B_1 magnetic field settings. The resulting fitting curve is also shown in Fig. 2(a). From the peak frequency $\nu_L = 6217(3)$ kHz, a result $\mu = 4.097(2)\ \mu_N$ was deduced. The error quoted here included an error in the B_0 field calibration, performed for the present β-NMR setup with a proton NMR probe, of $\Delta B_0 \leqslant 0.01$ mT, which was in fact negligibly small. The presently obtained μ value agrees with the reported value $\mu = 4.088(5)\ \mu_N$ [9] within the experimental error. From the resonance amplitude the spin polarization of ^{33}Al was determined to be $P \sim -2.0(5)\%$, assuming $A_\beta \sim 0.89$, as deduced from the experimentally known β-decay branching ratios [10].

In Figs. 2(b) and (c) the measured R/R_0 ratios for the ^{33}Al in α-Al_2O_3 single crystal are shown as a function of the quadrupole frequency ν_Q (the β-NQR spectrum). In principle, the resonance width of AFP-NMR spectra becomes approximately a bin width of the swept frequency. The observed widths of the obtained NQR spectra are, however, much broader than $\Delta\nu_Q = 485(176)$ kHz of a wide (narrow) ν_Q-window scan. By fitting the spectrum of the wide ν_Q-window scan shown in Fig. 2(b) to a Gaussian function $G_\sigma(\nu_Q)$ of Eq. (4), a substantially broader width 1.3(2) MHz (FWHM), calculated from the resulting $\sigma = 564(97)$ kHz, was obtained, where σ, as well as a and $\nu_Q{}^{(0)}$, were treated as free

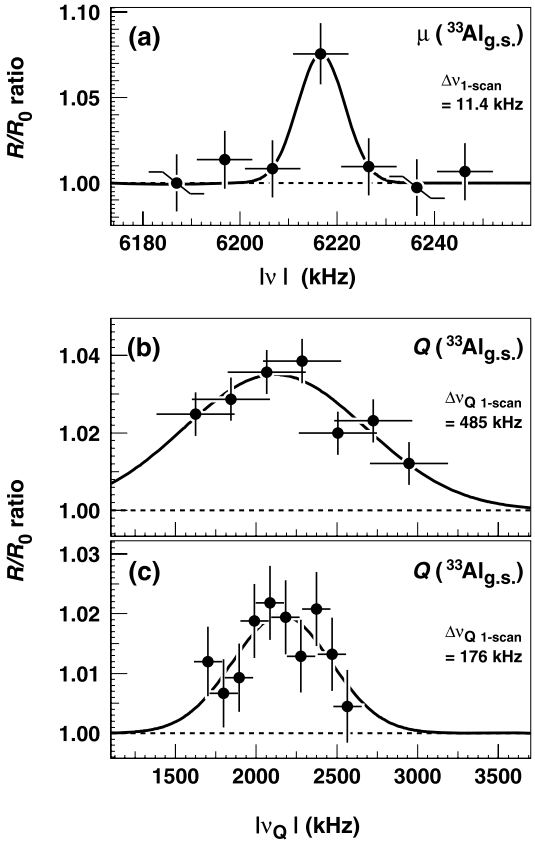

Fig. 2. (a) The NMR spectrum obtained for the ground state of ^{33}Al in a Si crystal. (b), (c) The NQR spectra obtained in an α-Al_2O_3 crystal with wide and narrow ν_Q-window scans. The ordinate of each spectrum shows a double ratio R/R_0, where R denotes the up/down ratio of the β-ray counts measured with application of the B_1 field for the quadrupole coupling frequency ν_Q, and R_0 the up/down ratio without the B_1 field. The vertical bar attached to the data point represents the statistical error due to β-counting statistics, while the horizontal bar indicates the width of the ν (ν_Q) frequency sweeps. The results of the least-χ^2 fitting analysis are shown by solid curves.

parameters to be determined through the fitting. The obtained parameter $\nu_Q{}^{(0)} = 2116(73)$ kHz represents the position of the peak, from which the quadrupole coupling constant eqQ/h will be deduced. According to a numerical simulation, $\sigma_{AFP} = 209$ kHz is expected as a width caused by the AFP spin reversal process, in which further line-shape broadening effects, e.g., due to the fluctuation of an electric field gradient q are not included. As a result, an extra broadening $\sigma_{extra} = 524$ kHz is needed in order to reproduce the observed $\sigma = 564$ kHz. The origin of σ_{extra} has not yet been well understood. Although an externally implanted Al ion would most likely stop at the site of the same element in the host crystal, there may be a possibility that some fraction of the implanted ions stop at other, metastable, sites. Also, some of the implanted ions might stop at a site of ^{27}Al atom that is accompanied by a near-by lattice defect produced by implantation, thus leading to a shifted NQR resonance. In these cases the NQR spectrum would show a broadened peak. In the present analysis such effects are expressed as a non-zero value of σ_{extra}. We therefore took into account the extra width determined in the fitting, $\sigma_{extra} = 524$ kHz, as an independent systematic error. Thus, an experimental error $\delta\nu_Q{}^{(0)} = \pm 77$ (stat) $\pm$ 524 (sys) kHz was assigned to the peak frequency $\nu_Q{}^{(0)} = 2116$ kHz, where an uncertainty from the eq value, $\delta\nu_Q = 14$ kHz, and that from a θ setting error, 1.1 kHz, were also included. The same fitting procedure was then applied to a narrow ν_Q-window scan

spectrum shown in Fig. 2(c), with a resulting peak frequency $\nu_Q^{(0)} = 2159(46)$ kHz. For the obtained peak an extra broadening effect was observed again with $\sigma = 263$ kHz at this time, and was regarded to represent a systematic error in the obtained $\nu_Q^{(0)}$. Thus, the peak frequency was determined to be $\nu_Q^{(0)} = 2159 \pm 46$ (stat) ± 263 (sys) kHz. The $\nu_Q^{(0)}$'s determined from the wide and narrow ν_Q scans agree very well. We have obtained a quadrupole coupling constant $|\nu_Q| = |eqQ/h| = 2.16(27)$ MHz from the narrow ν_Q scan, in which the observed extrabroadening effect is smaller. The Q moment of ^{33}Al is deduced from the relation $|Q(^{33}\mathrm{Al})| = |Q(^{27}\mathrm{Al}) \cdot \nu_Q(^{33}\mathrm{Al})/\nu_Q(^{27}\mathrm{Al})|$, where $Q(^{27}\mathrm{Al})$ and $\nu_Q(^{27}\mathrm{Al})$ denote the Q moment of ^{27}Al and the quadrupole coupling constant of ^{27}Al in α-Al_2O_3, respectively. By inserting the reported values $Q(^{27}\mathrm{Al}) = 146.6(10)$ $e$mb [29] and $\nu_Q(^{27}\mathrm{Al}) = 2389(2)$ kHz [30], the ground-state Q moment for ^{33}Al has been determined as $|Q_{\mathrm{exp}}(^{33}\mathrm{Al})| = 132(16)$ $e$mb.

Before turning to a closer examination of $|Q_{\mathrm{exp}}(^{33}\mathrm{Al})|$, a few remarks should be made concerning its μ moment. In the study of the μ-moment measurement of ^{33}Al [9], $\mu_{\mathrm{exp}}(^{33}\mathrm{Al})$, it was reported that $|\mu_{\mathrm{exp}}(^{33}\mathrm{Al})|$ differs from the theoretical μ of the shell-model calculation with the USD interaction [31] by 3.9%, and that this difference can be explained by the admixture of pf-intruder configurations of at least 25%. This statement is also supported by a large scale shell model calculation in the Monte Carlo Shell Model (MCSM), with the SDPF-M interaction [32]. This calculation reproduces $|\mu_{\mathrm{exp}}(^{33}\mathrm{Al})|$ within a 0.4% difference, in which the admixture of 63% intruder configurations is predicted. The above observation also indicates that $\mu_{\mathrm{exp}}(^{33}\mathrm{Al})$ is rather insensitive to the pf admixture. This insensitivity seems reasonable if configurations, in which two neutrons are excited to the pf orbit, are considered. The contribution from these configurations to the μ moment is a second-order correction, while the contribution to the Q moment is a first-order effect. Reflecting this, the theoretical value of $Q(^{33}\mathrm{Al})$ in the SDPF-M model largely differs from that in the USD model, by $\Delta Q(^{33}\mathrm{Al}) = 41\%$, in contrast to the small difference $\Delta\mu(^{33}\mathrm{Al}) = 4.3\%$[6] in the theoretical values of $\mu(^{33}\mathrm{Al})$ between the two models. A similar example is the case of ^{29}Na, in which both the USD and SDPF-M calculations well reproduce the experimental μ moment, while their theoretical Q moments differ by 30% from each other. The experimental Q agrees well with the SDPF-M prediction [34].

The obtained $|Q_{\mathrm{exp}}(^{33}\mathrm{Al})|$, together with those reported for other odd-aluminum isotopes [20,22,29], is plotted as a function of mass number in Fig. 3(a). The values of the ^{27,31}Al and ^{33}Al $I = 5/2$ ground states are all very similar, around 130–140 $e$mb. However, if $N = 20$ is a well-developed shell gap, then one would expect a much smaller quadrupole moment for ^{33}Al, as its quadrupole moment would be only determined by the odd-proton configuration (thus including only proton–proton correlations). No mixing of neutron configurations in the ground state wave function can occur if the $N = 20$ shell is completely filled and excitations across $N = 20$ are excluded. When opening the $N = 20$ shell, as in ^{27}Al and ^{31}Al, an increase in the quadrupole moment occurs due to proton–neutron and neutron–neutron correlations in the sd shell. This is nicely shown by the USD shell model calculations [31,35], which are performed in the sd shell model space for both protons and neutrons. As in our earlier studies [20,22,28], isospin-dependent effective charges were used for protons and neutrons [36].[7] Independent on the used effective interaction (USD, USDA or USDB [37]), a similar trend is predicted for the odd-Al quadrupole moments, in agreement with the observed values for ^{27}Al and ^{31}Al. However, the predicted value for ^{33}Al (95 $e$mb) is much smaller than the observed one (132(16) $e$mb), suggesting that neutron–neutron and/or neutron–proton correlations are required to reproduce the increased ^{33}Al quadrupole moment. Thus opening up the sd shell is needed, and excitations of neutrons into the fp shell, across the $N = 20$ gap, need to be taken into account.

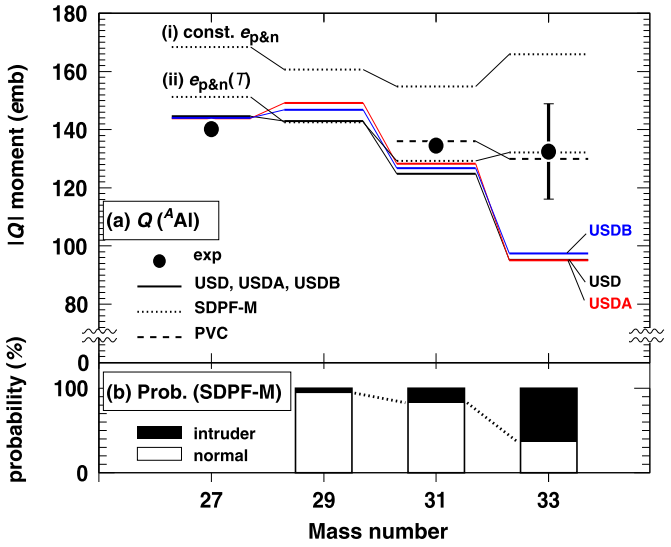

Fig. 3. (a) Experimental (solid circles) and theoretical (lines) Q moments of odd-mass neutron-rich aluminum isotopes as a function of mass number. The data for $A = 31$ is plotted by taking a weighted average of the results from Refs. [20] and [22]. Theoretical values are obtained from shell model calculations with USD interactions using isospin-dependent effective charges (solid line). Theoretical values of Monte Carlo Shell Model (SDPF-M), for which (i) constant effective charges and (ii) isospin-dependent effective charges are adopted, and a particle-vibration coupling model (PVC) are also shown by dotted and dashed lines, respectively. (b) The probabilities for normal and intruder configurations predicted by SDPF-M are shown.

In Fig. 3(a) theoretical Q moments predicted by the MCSM, with the SDPF-M interaction [32] and the constant effective charges adopted in the study of Na isotopes [34], are shown by a dotted line (i). Also, the probability for the pf intruder configuration predicted by the MCSM is shown in Fig. 3(b). In fact, the predicted pf intruder probability increases from 5–10% for the cases of $^{29-32}$Al to 63% for the ^{33}Al case, suggesting a weakening of the $N = 20$ shell closure. Accordingly, the theoretical Q moment for ^{33}Al is large, $Q_{\mathrm{MCSM}}(^{33}\mathrm{Al}) = 166$ $e$mb. The observed Q, $|Q_{\mathrm{exp}}(^{33}\mathrm{Al})| = 132(16)$ $e$mb, falls in between the USD and MCSM values. We note, however, that MCSM well reproduces $|Q_{\mathrm{exp}}(^{33}\mathrm{Al})|$ if we adopt the above noted isospin-dependent effective charges, as shown by a dotted line (ii). The situation is definitely different from the neighboring nucleus ^{31}Al, for which the μ [17] and Q [20,22] moments as well as the level structure [17] are well reproduced by the sd shell model.

The above observation indicates that the ^{33}Al ground state is mixed with pf-intruder configurations whereas the ^{31}Al ground state is not. In a next step, we can investigate whether the admixture of pf-intruder configurations is caused by a static nuclear deformation. Assuming an axially symmetric static deformation with the nuclear spin along the symmetry axis, the spectroscopic

[6] The quoted value of difference $\Delta\mu(^{33}\mathrm{Al}) = 4.3\%$ is for a case when the free-nucleon M1 operators are adopted, as in Ref. [9]. If instead the effective operators of Ref. [33] are adopted, $\Delta\mu(^{33}\mathrm{Al})$ becomes 6.7% which is still small compared to $\Delta Q(^{33}\mathrm{Al})$.

[7] Specifically, we took effective charges of proton (neutron) e_p (e_n) = 1.10 (0.56), 1.09 (0.53), 1.07 (0.44), and 1.05 (0.38) for $^{27, 29, 31, 33}$Al isotopes, respectively.

quadrupole moment Q is related to its intrinsic quadrupole moment Q_0 through a relation:

$$Q = \frac{3K^2 - I(I+1)}{(I+1)(2I+3)} Q_0 \tag{5}$$

with K the projection of the nuclear spin I on the deformation symmetry axis (thus $K = I$). The intrinsic quadrupole moment of an ellipsoidal charge distribution can then be related to the quadrupole deformation parameter β as follows:

$$Q_0 = (3/\sqrt{5\pi}) Z R^2 \beta (1 + 0.36\beta + \cdots)$$
$$\left(R = 1.2A^{1/3}\right) \tag{6}$$

Using these expressions, we find similar deformation parameters for ^{31}Al and ^{33}Al, respectively $\beta = 0.25$ and 0.24. This similarity between these β values suggests that the admixture of *pf*-intruder configurations in ^{33}Al does not receive significant influence of the nuclear deformation, since such an admixture is considered to be small in ^{31}Al.

Fig. 3(a) includes the prediction from the mean field approach [38] as indicated by a dashed line: The structure of ^{33}Al was treated in a microscopic particle-vibration coupling (PVC) model in which the coordinate-space Skyrme–Hartree–Fock–Bogoliubov and quasiparticle-random-phase approximations were employed. In this model, the ^{33}Al ground state was described as a proton single-hole state $(\pi d_{5/2})^{-1}$ coupled to a ^{34}Si core to form $I^\pi = 5/2^+$.

The PVC Hamiltonian is diagonalized in a model space consisting of the $(\pi d_{5/2})^{-1}$ hole state coupled to the quadrupole vibrational states in ^{34}Si. The resulting ^{33}Al ground-state wavefunction involves a substantial neutron mean occupation number in the *pf* orbit of $\sim$0.8. This feature is inherited from the $I^\pi = 0^+$ core state of ^{34}Si. It is interesting to note that a spherical shape is predicted for the ^{34}Si core state in spite of the substantial amplitude of intruder configurations, where the neutron pairing, instead of the static deformation, associated with the weakening of the $N = 20$ magic number plays an important role. Also, a predicted theoretical Q moment $Q_{\mathrm{PVC}}(^{33}\mathrm{Al}) = 130$ *e*mb [38] with this wavefunction reproduces excellently the presently obtained $|Q_{\mathrm{exp}}(^{33}\mathrm{Al})|$.

In summary, the ground-state Q moment of ^{33}Al has been determined by the β-NQR method using the fragmentation-induced spin polarization. The obtained Q moment, $|Q_{\mathrm{exp}}(^{33}\mathrm{Al})| = 132(16)$ *e*mb, shows a significant excess from the prediction of the USD shell model calculation. The large Q is a clear signature that the $N = 20$ shell closure erodes in ^{33}Al. The structure of the ^{33}Al ground state was then investigated through the obtained $|Q_{\mathrm{exp}}(^{33}\mathrm{Al})|$ by comparing with theoretical values predicted from the large scale shell model MCSM and a particle-vibration coupling model treating the neutron pairing correlations in the ground state of ^{33}Al instead of the static nuclear deformation. A significant admixture of *pf* intruder configurations to the ^{33}Al ground state was needed in both theoretical approaches to explain the observed large Q.

Acknowledgements

The authors thank the staff of GANIL for their support during the experiment. This work was partly supported by the JSPS KAKENHI (22340071), by the JSPS and MAEE under the Japan–France Integrated Action Program (SAKURA), by the French–Japanese International Associated Laboratory for Nuclear Structure Problems (LIA), and also financed by the European Community FP6 – Structuring the ERA – Integrated Infrastructure Initiative contract EURONS No. RII3-CT-2004-506065, by the FWO-Vlaanderen, by the IAP-programme of the Belgium Science Policy under grand number P6/23, and by Bulgarian National Science Fund, grant No. DID-02/16. The experiment was carried out under Experimental Program E437b.

References

[1] E.K. Warburton, J.A. Becker, B.A. Brown, Phys. Rev. C 41 (1990) 1147.
[2] C. Détraz, et al., Phys. Rev. C 19 (1979) 164.
[3] D. Guillemaud, et al., Nucl. Phys. A 426 (1984) 37.
[4] T. Motobayashi, et al., Phys. Lett. B 346 (1995) 9.
[5] G. Huber, et al., Phys. Rev. C 18 (1978) 2342.
[6] D.T. Yordanov, et al., Phys. Rev. Lett. 99 (2009) 212501.
[7] C. Thibault, et al., Phys. Rev. C 12 (1975) 644;
C. Détraz, et al., Nucl. Phys. A 394 (1983) 378.
[8] P.J. Woods, et al., Phys. Lett. B 182 (1986) 297;
N.A. Orr, et al., Phys. Lett. B 258 (1991) 29.
[9] P. Himpe, et al., Phys. Lett. B 643 (2006) 257.
[10] A.C. Morton, et al., Phys. Lett. B 544 (2002) 274.
[11] V. Tripathi, et al., Phys. Rev. Lett. 101 (2008) 142504.
[12] M. Yamagami, Nguyen Van Giai, Phys. Rev. C 69 (2004) 034301.
[13] N. Hinohara, et al., arXiv:1109.2060v1 [nucl-th].
[14] K. Sugimoto, A. Mizobuchi, K. Nakai, K. Matsuta, J. Phys. Soc. Jpn. 21 (1966) 213.
[15] K. Asahi, et al., Phys. Lett. B 251 (1990) 488.
[16] H. Okuno, et al., Phys. Lett. B 335 (1994) 29.
[17] D. Borremans, et al., Phys. Lett. B 537 (2002) 45.
[18] H. Ueno, et al., Phys. Lett. B 615 (2005) 186.
[19] P. Himpe, et al., Phys. Lett. B 658 (2008) 203.
[20] D. Nagae, et al., Phys. Rev. C 79 (2009) 027301.
[21] D. Kameda, et al., Phys. Lett. B 647 (2007) 93.
[22] M. De Rydt, et al., Phys. Lett. B 678 (2009) 344.
[23] M. De Rydt, et al., Nucl. Instr. Methods A 612 (2009) 212.
[24] A. Abragam, The Principle of Nuclear Magnetism, Clarendon, Oxford, 1961.
[25] D. Nagae, et al., Nucl. Instr. Methods B 266 (2008) 4612.
[26] P.M. Endt, R.B. Firestone, Nucl. Phys. A 633 (1998) 1.
[27] R. Brun, F. Carminati, CERN Application Software Group, GEANT3.2, CERN Program Library, Writeup Report No. W5013, 1994.
[28] H. Ogawa, et al., Phys. Rev. C 67 (2003) 064308.
[29] V. Kellö, et al., Chem. Phys. Lett. 304 (1999) 414.
[30] S.J. Gravina, P.J. Bray, J. Mag. Reson. 89 (1990) 515.
[31] B.H. Wildenthal, Prog. Part. Nucl. Phys. 11 (1984) 5.
[32] Y. Utsuno, et al., Phys. Rev. C 60 (1999) 054315.
[33] B.A. Brown, B.H. Wildenthal, Nucl. Phys. A 474 (1987) 290.
[34] Y. Utsuno, et al., Phys. Rev. C 70 (2004) 044307.
[35] B.A. Brown, A. Etchegoyen, W.D.M. Rae, OXBASH, MSU Cyclotron Laboratory Report No. 524, 1986.
[36] A. Bohr, B.R. Mottelson, Nuclear Structure, vol. II, World Scientific, Singapore, 1998.
[37] W.A. Richter, S. Mkhize, B.A. Brown, Phys. Rev. C 78 (2008) 064302.
[38] K. Yoshida, Phys. Rev. C 79 (2009) 054303.